



# Determination of molecular mass distribution of amylopectin using asymmetrical flow field-flow fractionation

Shazia Juna<sup>a</sup>, Peter A. Williams<sup>a,\*</sup>, Simon Davies<sup>b</sup>

<sup>a</sup> Centre for Water Soluble Polymers, Glyndwr University, Plas Coch, Mold Road, Wrexham LL11 2AW, UK

<sup>b</sup> National Starch, Wilton Centre, Wilton, Redcar TS10 4RF, UK

## ARTICLE INFO

### Article history:

Received 2 April 2010

Received in revised form 25 August 2010

Accepted 27 September 2010

Available online 4 November 2010

### Keywords:

Waxy maize starch

Amylopectin

Asymmetrical flow field-flow fractionation

High pressure microwave vessel

Light scattering

## ABSTRACT

The molar mass ( $M_w$ ), radius of gyration ( $R_g$ ), diffusion co-efficient ( $D$ ), and hydrodynamic radius ( $R_h$ ) of amylopectin (waxy maize starch) has been determined using asymmetrical flow field-flow fractionation coupled with multi-angle light scattering and refractive index detectors (AF4/MALS/RI). A high pressure microwave vessel (HPMV) was used to dissolve amylopectin in 1 M KSCN. The effect of varying the flow rates on the  $M_w$  and  $R_g$  distributions of amylopectin were investigated to determine the optimum flow rates. The average  $M_w$  and  $R_g$  values of amylopectin determined using the Berry and Debye equations.  $D$  and  $R_h$  values were determined directly from the AF4 retention times and compared to values obtained by dynamic light scattering.

© 2010 Elsevier Ltd. All rights reserved.

## 1. Introduction

Starch is an abundant material and is obtained commercially mainly from maize, potato, wheat, tapioca and rice (Murphy, 2000). It occurs in the form of granules, which have varying degrees of structural order and consists of two polysaccharides, namely amylose and amylopectin. Amylose consists of linear  $\alpha$ -(1,4)-linked glucopyranose chains with very little branching (10 branch points per molecule), while amylopectin also contains sequences of  $\alpha$ -(1,4)-linked glucopyranose units, however, it has extensive branching via  $\alpha$ -(1,6) linkages. The molecular mass of amylose may range from  $10^5$  to  $10^6$  g/mol while that for amylopectin may range from  $10^7$  to  $10^8$  g/mol (Banks & Greenwood, 1975; Murphy, 2000). Considerable efforts made over the last thirty years or so to determine the molecular mass distribution and radius of gyration,  $R_g$  of starch using various techniques such as Size Exclusion Chromatography (SEC) (Bello-Perez, Roger, Baud, & Colonna, 1998; Fishman & Hoagland, 1994; Fishman, Rodriguez, & Chau, 1996; Han & Lim, 2004a, 2004b; Han, Lim, & Lim, 2005; Tetchi, Rolland-Sabaté, Amani, & Colonna, 2007; Yoo & Jane, 2002), Static Light Scattering (SLS) (Aberle, Burchard, Vorwerg, & Radosta, 1994; Bello-Perez, Paredes-Lopez, Roger, & Colonna, 1996; Bello-Perez, Roger, Colonna, & Paredes-Lopez, 1998; Elfstrand et al., 2004;

Millard, Wolf, Dintzis, & Willet, 1999; Roger, Bello-Perez, & Colonna, 1999; Vorwerg & Radosta, 1995; Yang et al., 2006) and Flow Field Flow Fractionation (FFFF) (Bowen et al., 2006; Hanselmann, Burchard, Ehrat, & Widmer, 1996; Roger, Boud, & Colonna, 2001; Rolland-Sabate, Colonna, Mendez-Montealvo, & Planchot, 2007; van Bruijnsvoort, Wahland, Nilsson, & Kok, 2001), as shown in Table 1. However, SEC is incapable of achieving the desired resolution for very large molecules such as amylopectin due to shear scission (Cave, Seabrook, Gidley, & Gilbert, 2009; Gidley et al., 2010). Complete dissolution of starch is required to determine the molar mass and its limited solubility in water is a major obstacle for its characterization. Researchers have adopted various strategies and protocols to disrupt the crystalline structure of starch to facilitate dissolution. In order to produce meaningful data it is necessary to completely disaggregate the amylopectin and amylose molecules within the granules without inducing molecular degradation. The dissolution methods that have been adopted include: solvation in DMSO (Bello-Perez et al., 1996; Han & Lim, 2004a; Han et al., 2005; Millard et al., 1999), treatment with alkali or acid (Han & Lim, 2004b; Yang et al., 2006), high pressure treatment (Bowen et al., 2006), high temperature treatment (Aberle et al., 1994; Bultosa, Hamaker, & BeMiller, 2008; Elfstrand et al., 2004; Hanselmann et al., 1996; van Bruijnsvoort et al., 2001; Vorwerg & Radosta, 1995; Yoo & Jane, 2002), sonication (Jackson, Waniska, & Rooney, 1988), homogenization (Modig, Nilsson, Bergensthal, & Wahlund, 2006), ionic liquid (Stevenson, Biswas, Jane, & Inglett, 2007) and high pressure microwave vessel (HPMV) (Bello-Perez, Roger, Baud, et al., 1998; Bello-Perez, Roger, Colonna, et al., 1998;

\* Corresponding author.

E-mail address: [p.a.williams@glyndwr.ac.uk](mailto:p.a.williams@glyndwr.ac.uk) (P.A. Williams).

**Table 1**  
Literature  $M_w$  and  $R_g$  values for waxy maize starch.

Dissolution process	Method	$M_w$ ( $\times 10^6$ g/mol)	$R_g$ (nm)	$R_h$ (nm)	Ref.
DMSO, heated for 1 h at 90–100 °C, stored for various time periods	SEC/MALS/RI	171–254	226–244	–	Han and Lim (2004a)
90% DMSO/H <sub>2</sub> O, heated for 50 min in hot H <sub>2</sub> O bath	SEC/MALS/RI	254	241	–	Han et al. (2005)
90% DMSO–H <sub>2</sub> O	SLS & DLS	560	342	348	Millard et al. (1999)
DMSO, heated for 1 h at 90–100 °C, stored for 8 h	SLS	274	255	–	Han et al. (2005)
10% DMSO, 90% H <sub>2</sub> O	SLS & DLS	53	242	58	Bello-Perez et al. (1996)
1 M NaOH, rt, vortexed for various time periods	SEC/MALS/RI	88–185	198–215	–	Han and Lim (2004b)
0.5 M NaOH stirred for 18 h, various temperatures	SLS, DLS	129–530	223–276	172–282	Yang et al. (2006)
Boiled in water (30 min)	SEC/MALS/RI	830	372	–	Yoo and Jane (2002)
Autoclaved at 155 °C for 20 min	SLS	77	234	–	Aberle et al. (1994)
Heated at 135 °C for 20 min	SLS	77	–	–	Vorwerg and Radosta (1995)
Heated in 0.1 M NaNO <sub>3</sub> at 120 °C, 15 min	SLS	47	62	–	Elfstrand et al. (2004)
Heated in H <sub>2</sub> O	AF4/MALS/RI	10–1000	Over 300	–	van Bruijnsvoort et al. (2001)
Autoclaved at 175 °C, 20–60 min	SdFFF/MALS	38–360	121–320	–	Hanselmann et al. (1996)
Heated at 140–50 °C in a pressure cell	AF4/MALS/RI	4092	–	–	Bowen et al. (2006)
Heated for 90 s, (HPMV 700 W)	SEC/MALS/RI	19.5	81	–	Fishman and Hoagland (1994)
Heated for 80 s (HPMV 700 W)	SEC/MALS/RI	26	76	–	Fishman et al. (1996)
Heated for 35 s, stored for 0–24 h (HPMV 900 W)	SEC/MALS/RI	140–200	220–234	–	Bello-Perez, Roger, Baud, et al. (1998)
Heated for 35 s (HPMV 900 W)	SEC/MALS/RI	318	241	–	Tetchi et al. (2007)
Heated for 35 s, stored for 0–72 h (HPMV 900 W)	SLS, DLS	110–270	200–259	183–203	Bello-Perez, Roger, Colonna, et al. (1998)
Heated for 35–90 s (HPMV 900 W)	SLS, DLS	78–270	170–260	148–221	Roger et al. (1999)
Heated for 35 s (HPMV 900 W)	FFFF/MALS/RI	450	334	–	Roger et al. (2001)
Heated for 40 s (HPMV, 900 W)	AF4/MALS/RI	318	241	–	Rolland-Sabate et al. (2007)

Fishman & Hoagland, 1994; Fishman et al., 1996; Roger et al., 1999; Roger et al., 2001; Rolland-Sabate et al., 2007; Tetchi et al., 2007).

This paper describes experiments undertaken to determine the molecular mass distribution of amylopectin from waxy maize starch sample using AF4/MALS/RI.

### 1.1. AF4/MALS/RI

The theory of AF4 has been described elsewhere in the literature (Andersson, Wittgren, & Wahlund, 2001; Bowen et al., 2006; Hanselmann et al., 1996; Roger et al., 2001; Rolland-Sabate et al., 2007; van Bruijnsvoort et al., 2001; Viebke & Williams, 2000; Wahlund, 2000; Wittgren & Wahlund, 1997). The fractionation of molecules takes place in a thin channel, which consists of a permeable lower wall, known as the accumulation wall, and an upper impermeable solid wall (Viebke & Williams, 2000). The separation of the molecules is governed by the differences in the diffusion coefficient  $D$ . The diffusion coefficient,  $D$ , of the molecules can be determined directly from AF4 as shown in Eq. (1) below, where  $t^0$  is the void time,  $F_{cr}$  is the cross flow,  $w$  is the channel thickness,  $V^0$  is the geometric void volume, and  $t_r$  is the retention time (Viebke & Williams, 2000).

$$D = \frac{t^0 F_{cr} w^2}{6V^0} \times \frac{1}{t_r} \quad (1)$$

Void time  $t^0$  is calculated using Eq. (2) (Wahlund, 2000).

$$t^0 = \frac{V^0}{F_{cr}} \ln \left\{ 1 + \frac{F_{cr}}{F_{ch}} \left[ 1 - \frac{w(b_0 z - ((b_0 - b_L)/2L)z^2 - y)}{V^0} \right] \right\} \quad (2)$$

The geometric void volume,  $V^0$  is determined from the channel parameters. The channel thickness,  $w$  is determined experimentally,  $b_0$  and  $b_L$  are the breadths at the channel inlet and outlet respectively,  $z$  is the distance between the channel inlet and the focusing point,  $y$  is the channel area lost by the tapered inlet,  $F_{cr}$  is the cross flow rate,  $F_{ch}$  is the channel flow rate and  $L$  is the channel length.

The hydrodynamic radius,  $R_h$  of the molecule is related to  $D$  according to the Stokes–Einstein relationship (Andersson, Wittgren, & Wahlund, 2003),

$$R_h = \frac{kT}{6\pi\eta D} \quad (3)$$

$R_h$  can therefore be determined directly from the retention time as shown in Eq. (4), where,  $k$  is Boltzmann's constant,  $T$  is the temperature (K),  $F_{cr}$  is the cross flow,  $\eta$  the viscosity coefficient of the solvent and  $t_r$  is the retention time (Wahlund, 2000).

$$R_h = \frac{kTV^0}{\pi\eta t^0 F_{cr} w^2} \times t_r \quad (4)$$

The retention of the molecules is dependent on the cross flow ( $F_{cr}$ ) and channel flow ( $F_{ch}$ ) ratio,  $F_{cr}/F_{ch}$  which may be determined from Eq. (5), if the diffusion coefficient of the molecule is known (Wahlund, 2000).

$$\frac{F_{cr}}{F_{ch}} = \frac{\exp(6Dt_r/w^2) - 1}{A} \quad (5)$$

In online multi-angle laser light scattering (MALS) the scattered light is measured at various angles ranging from 26° to 143°, the excess Rayleigh ratio is extrapolated to zero angle using the Berry (Eq. (6)) and Debye (Eq. (7)) fits (Andersson et al., 2003), where  $c$  is the concentration of the macromolecules,  $M_w$  is the weight-average molar mass,  $P(\theta)$  is the particle scattering function,  $R_\theta$  is the excess Rayleigh ratio,  $K$  an optical constant,  $\lambda_0$  is the wavelength of the laser in vacuum.

$$\frac{Kc}{R_\theta} = \frac{1}{M_w} + \frac{16\pi^2}{3\lambda^2} \times R_g^2 \times \sin^2 \left( \frac{\theta}{2} \right) \quad (6)$$

$$\sqrt{\frac{Kc}{R_\theta}} = \sqrt{\frac{1}{M_w} + \frac{16\pi^2}{3\lambda^2} \times R_g^2 \times \sin^2 \left( \frac{\theta}{2} \right)} \quad (7)$$

The molecular mass of the macromolecule is obtained from the intercept and the radius of gyration from the gradient.

## 2. Materials and methods

A sample of waxy maize starch was provided by National Starch. Amylopectin Azure (Sigma–Aldrich; Gillingham, UK), a blue-colored water-soluble potato amylopectin starch was employed to visualize the focusing step. Bovine serum albumin (BSA) was also obtained from Sigma–Aldrich, Gillingham, UK to calibrate the channel thickness.

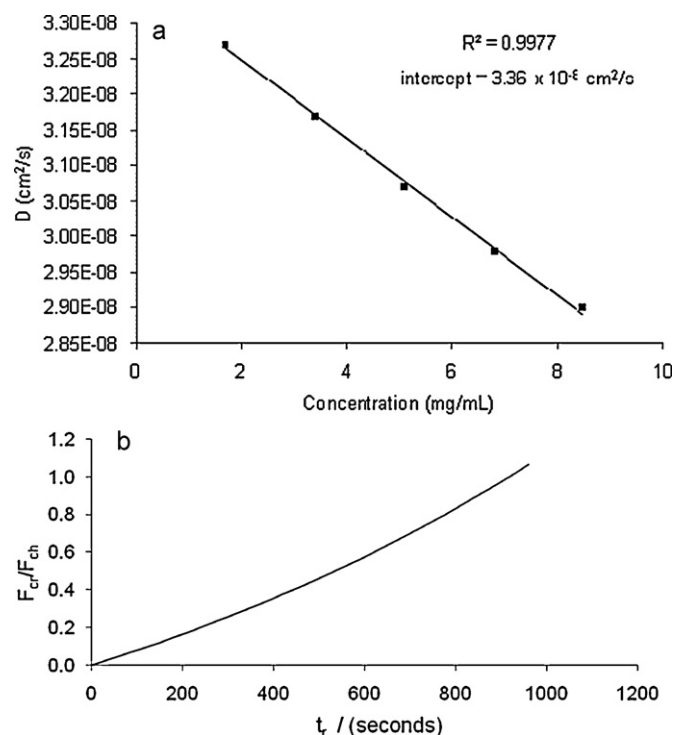


**Fig. 1.** (a) Plot of  $D$  as a function of waxy maize starch concentration determined using DLS. (b)  $F_{cr}/F_{ch}$  as a function of  $t_{cr}$ .

### 2.1. Dissolution using a high pressure microwave vessel (HPMV)

HPMV has been employed by a number of researchers for the dissolution of starch (Bello-Perez, Roger, Baud, et al., 1998; Bello-Perez, Roger, Colonna, et al., 1998; Fishman & Hoagland, 1994; Fishman et al., 1996; Roger et al., 1999, 2001; Rolland-Sabate et al., 2007; Tetchi et al., 2007) and polysaccharides (Ratcliffe, Williams, Viebke, & Meadows, 2005). Pregelatinisation of waxy maize starch samples was carried out by dissolving each sample in DMSO (95%), stirring for 12 h and then precipitating with ethanol. The pregelatinised waxy maize starch sample was dried at room temperature. 20–30 mg of the pregelatinised waxy maize starch sample was left to stir in 50 ml of 1 M KSCN for 12 h, following which 20 ml of the solution was then transferred into the Teflon cup of a model 4782 polycarbonate HPMV (total volume 45 ml) (Parr Instrument Co., Moline, IL) and placed in a microwave oven (800 W) and heated at 90% power for 60 s. The HPMV was cooled in an ice bath for 1 h after which the solution was filtered through an 8  $\mu$ m cellulose nitrate filter.

### 2.2. AF4/MALS/RI

Starch solutions were analysed using AF4/MALS/RI. The eluent (0.035 M KSCN) was passed through a vacuum degasser (Cambridge Scientific Instruments Ltd., Ely, UK) into the Flow Box P 2.1 (ConSensus, Ober-Hilbersheim, Germany) and then through a 0.22  $\mu$ m inline filter (Millipore (U.K.) Ltd., Watford, UK) into the Control-Box V3 valve box (Control-Box V3, ConSensus, Germany) before entering the aFFFF channel (ConSensus, Ober-Hilbersheim, Germany). The dimensions of the channel were 320 mm  $\times$  100 mm  $\times$  145 mm, and the area of the accumulation wall was 36.09 cm<sup>2</sup>. A polysulphone membrane, with a  $M_w$ -cut-off of 10 kDa (ConSensus, Ober-Hilbersheim, Germany), and a 190  $\mu$ m spacer were employed. The sample was injected through a ChemInert<sup>®</sup> injection valve (VICI Valco Instruments Ltd., Houston, Texas) with a sample loop volume of 100  $\mu$ l. The channel outlet was connected both to the Valve

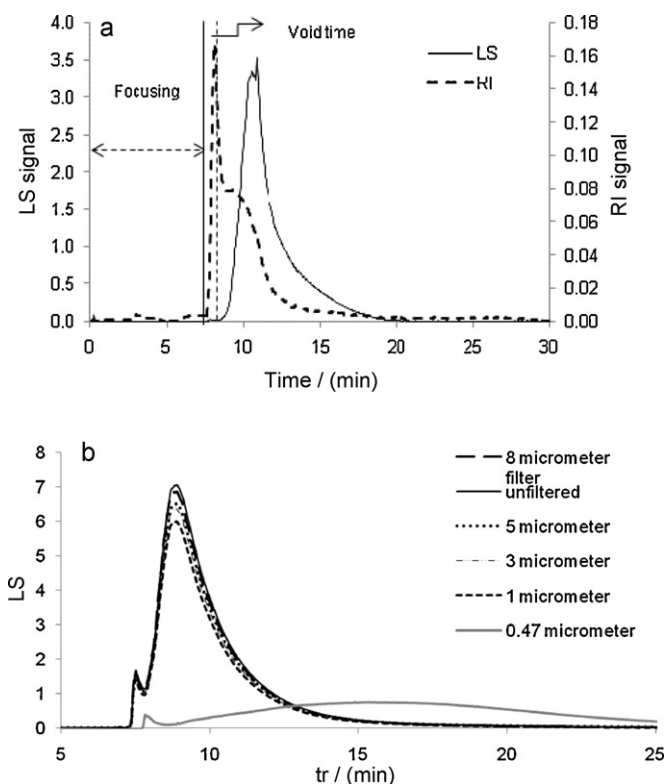


**Fig. 2.** (a) LS and RI as a function of time for waxy maize starch. The data corresponding to focusing and void time were not included in the determination of  $M_w$  and  $R_g$  of amylopectin. (b) LS signal as a function of  $t_{cr}$  for waxy maize starch solutions filtered through 8  $\mu$ m, 5  $\mu$ m, 3  $\mu$ m, 1  $\mu$ m and 0.47  $\mu$ m cellulose nitrate filters.

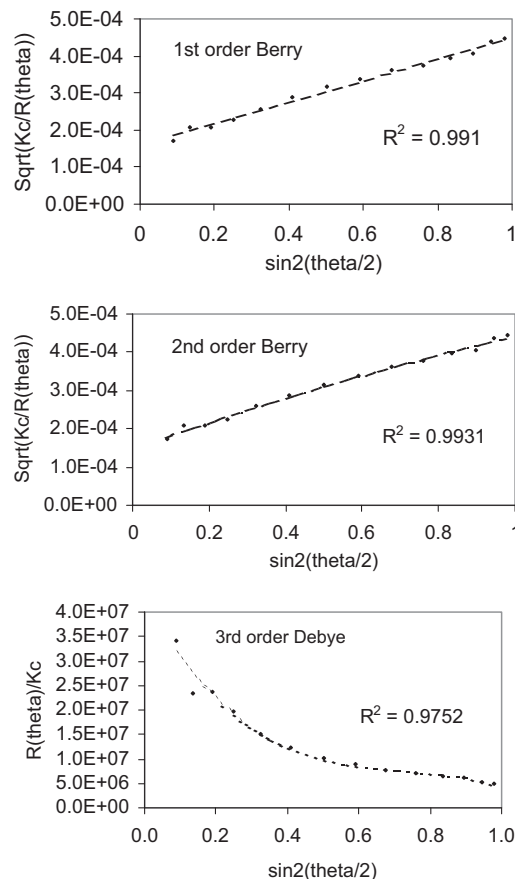


**Fig. 3.** Comparison of Debye and Berry fits for waxy maize starch.

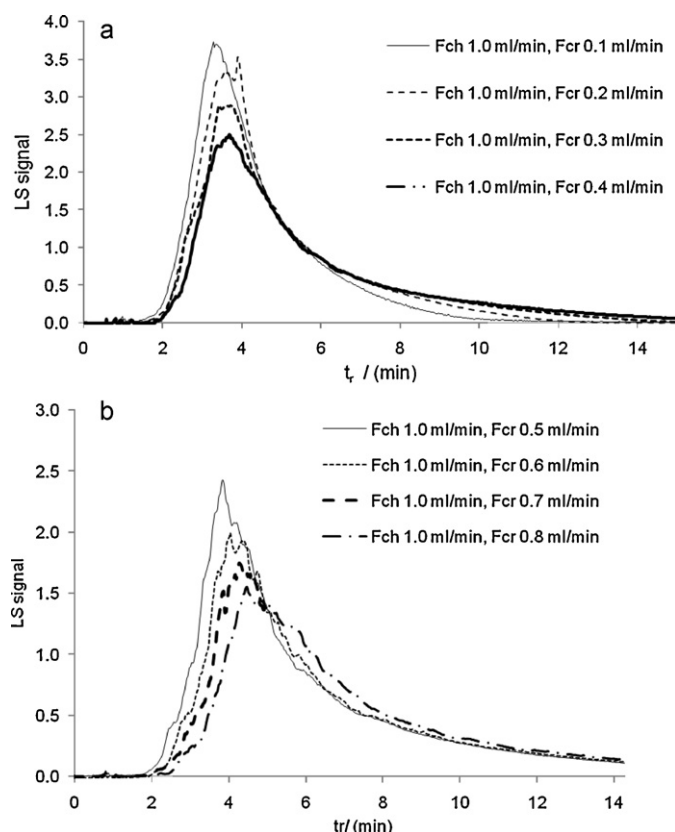


**Fig. 4.** (a) Effect of varying  $F_{cr}$  from 0.1 to 0.4 ml/min at a fixed  $F_{ch}$  rate of 1.0 ml/min upon LS peaks. (b) Effect of varying  $F_{cr}$  from 0.5 to 0.8 ml/min at a fixed  $F_{ch}$  rate of 1.0 ml/min upon LS peaks.

Box and the detectors. The flow rates were controlled employing WinFFF.Control V.30 software (ConSensus, Ober-Hilbersheim, Germany). The on-line detectors employed were multi-angle laser light scattering Wyatt Dawn<sup>®</sup> EOS ( $\lambda = 690$  nm) (Wyatt Technology Corporation, Santa Barbara, CA) and the RI detector was an interferometric refractometer Optilab DSP (Wyatt Technology Corporation, Santa Barbara, CA). The results were collected and processed employing ASTRA for Windows 4.90 (Wyatt Technology Corporation, Santa Barbara, CA).

The channel thickness was calculated using Eq. (4) from experiments using BSA, which has a diffusion coefficient of  $5.96 \times 10^{-7}$  cm<sup>2</sup>/s at 294 K, and was found to be 165  $\mu$ m.

The RI detector was calibrated with sodium chloride. The calibration constant of  $2.369 \times 10^{-5}$  was employed to process the data. The MALS detector was calibrated with toluene, and the calibration constant determined was  $9.04 \times 10^{-6}$ . A  $dn/dc$  value of 0.156 was determined for the waxy maize starch in 0.035 M KSCN experimentally.

### 2.3. Analysis of waxy maize using AF4/MALS/RI

Aqueous solutions of waxy maize starch were prepared by heating for 60 s in the HPMV. The focusing time was determined by direct observation with amylopectin-azure solution and found to be 7 min. The eluent employed was 0.035 M KSCN with 0.05% NaN<sub>3</sub> filtered through a Millipore 0.2  $\mu$ m cellulose nitrate filter. A 100  $\mu$ l sample of waxy maize starch solution in 1 M KSCN was focused for 7 min, a  $F_{ch}$  rate of 2.5 ml/min and a  $F_{cr}$  rate of 2.4 ml/min was used. The separation of waxy maize starch molecules was studied for a range of channel flow,  $F_{ch}$ , and cross flow,  $F_{cr}$ , rates.

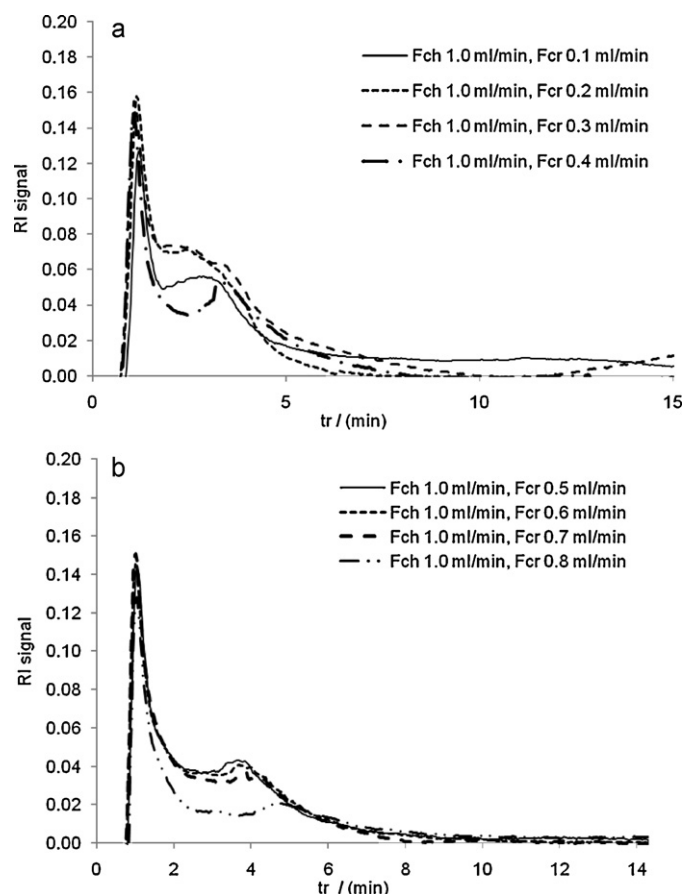


**Fig. 5.** (a) Effect of varying  $F_{cr}$  from 0.1 to 0.4 ml/min at a fixed  $F_{ch}$  rate of 1.0 ml/min upon RI peaks. (b) Effect of varying  $F_{cr}$  from 0.5 to 0.8 ml/min at a fixed  $F_{ch}$  rate of 1.0 ml/min upon RI peaks.

### 2.4. Determination of $D$ and $R_h$ of waxy maize starch using DLS

$D$  and  $R_h$  of waxy maize starch in 0.035 M KSCN was measured using the Malvern Zeta Nano ZS (Malvern Instruments Ltd., Malvern, UK). A stock solution of waxy maize starch (8.48 mg/ml in 1 M KSCN) was prepared by heating in a HPMV for 60 s followed by an hour of cooling in an ice bath. Further dilutions were prepared to yield five different concentrations ranging from 8.48 mg/ml to 1.69 mg/ml.  $D$  was determined at room temperature (21 °C) and plotted as a function of concentration. The diffusion coefficient at zero concentration,  $D_0$  was determined by extrapolation. The hydrodynamic radius  $R_h$  was determined using Eq. (3).

## 3. Results and discussion

The  $D$  values for waxy maize starch solutions at varying concentrations are presented in Fig. 1a.  $D_0$  was determined by extrapolation to zero concentration and was found to have a value of  $3.35 \times 10^{-8}$  cm<sup>2</sup> s<sup>-1</sup> which corresponds to an  $R_h$  value of 73 nm. Theoretical  $F_{cr}/F_{ch}$  values were calculated using Eq. (5) and the values are plotted in Fig. 1b. The sample will not elute if  $F_{cr}$  value is greater than that of  $F_{ch}$  value, therefore the value of  $F_{cr}/F_{ch}$  should not exceed 1. The resolution of the peak can be improved by fine tuning  $F_{cr}/F_{ch}$  values and the estimation of the  $t_r$  of the peak can also be undertaken from these values. At  $F_{cr}/F_{ch}$  values of 0.05–1.00, waxy maize starch peak is expected to elute within 16 min, as shown in Fig. 1b.



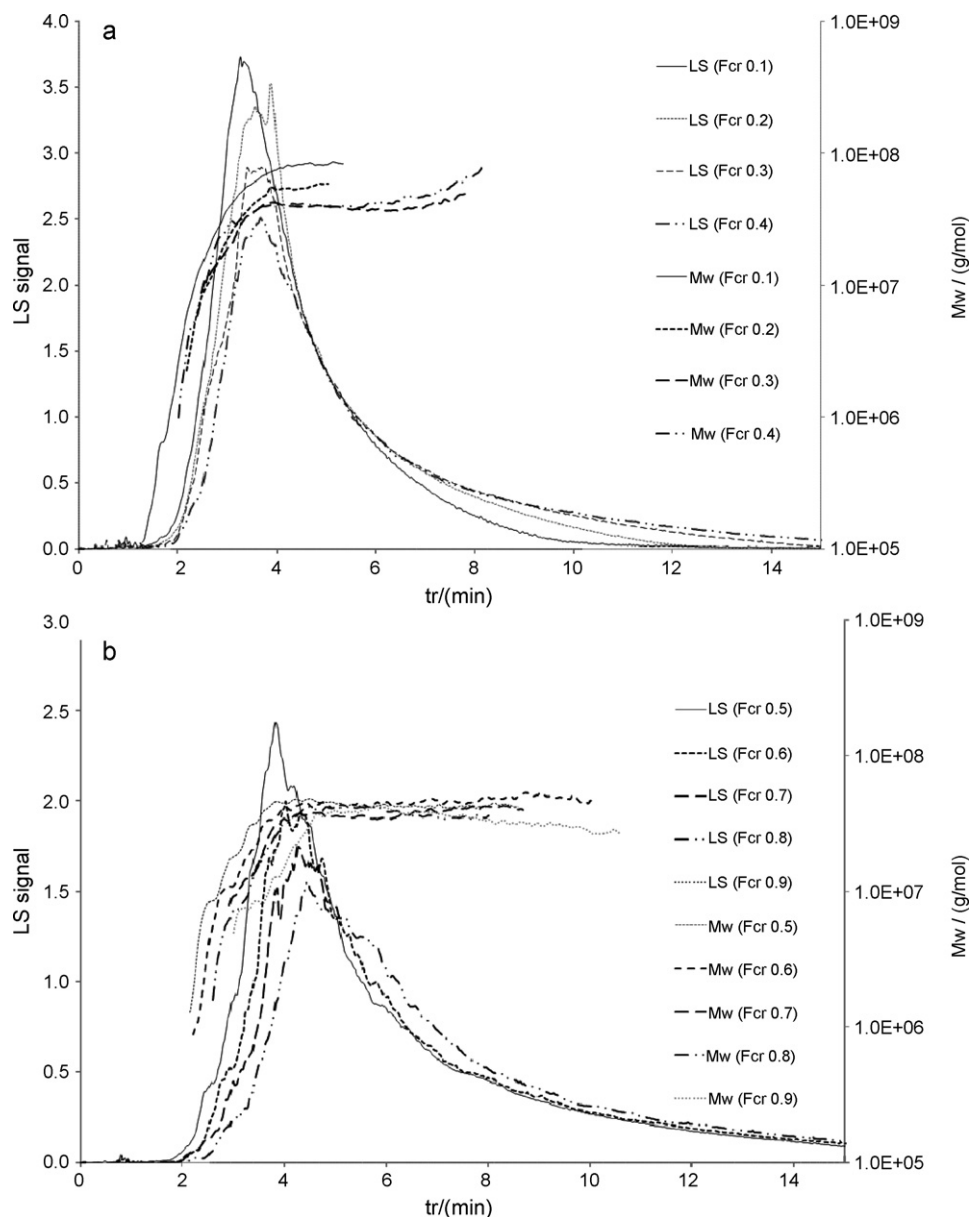


**Fig. 6.** (a)  $M_w$  as a function of  $t_r$  with LS peaks superimposed determined using the 1st order Berry fit obtained for waxy maize starch at a fixed  $F_{ch}$  rate of 1.0 ml/min with  $F_{cr}$  rates ranging from 0.1 ml/min to 0.4 ml/min. (b)  $M_w$  as a function of  $t_r$  with LS peaks superimposed determined using the 1st order Berry fit obtained for waxy maize starch at a fixed  $F_{ch}$  rate of 1.0 ml/min with  $F_{cr}$  rates ranging from 0.5 ml/min to 0.9 ml/min.

### 3.1. Typical elution profiles of waxy maize starch

A solution of waxy maize starch ( $2.76 \times 10^{-2}$  mg/ml) filtered through an  $8 \mu\text{m}$  cellulose nitrate filter was analysed with AF4/MALS/RI at  $F_{ch}$  of 1 ml/min and  $F_{cr}$  of 0.2 ml/min. The resultant LS and RI peaks are shown in Fig. 2a and indicate that the waxy maize starch is highly disperse, since the LS and RI peaks do not superimpose. The LS peak is very large in contrast to the RI peak. The former is due to the fact that the eluting molecules have a very high molecular mass and the latter is due to the fact that only a very low concentration of sample is used otherwise the light scattering signal becomes saturated. The LS signal increases steadily from 8.5 min and reaches a maximum intensity at around 10.5 min, thereafter the LS peak gradually decreases. Focusing of the waxy maize starch occurs for the initial  $\sim 7$  min. The overall pressure of the system during focusing increases from 10 bar to 18 bar and then returns to 10 bar in the transition from focusing to elution mode. The small spike in the RI peak observed at  $\sim 8$  min is an experimen-

tal artifact caused by the pressure drop and corresponds to the void time. The peak area corresponding the void peak was excluded from the analysis of light scattering and refractive index peak as shown in Fig. 2a.

### 3.2. Effect of filtration upon waxy maize starch AF4/MALS/RI elution profiles

The effect of filtration was investigated by filtering waxy maize starch solutions through  $8 \mu\text{m}$ ,  $5 \mu\text{m}$ ,  $3 \mu\text{m}$ ,  $1 \mu\text{m}$  and  $0.47 \mu\text{m}$  cellulose nitrate filters. These solutions were analysed by AF4/MALS/RI at a  $F_{ch}$  rate of 1.0 ml/min and a  $F_{cr}$  rate of 0.1 ml/min. The resultant LS peaks are shown in Fig. 2b. These were compared against LS peaks obtained with an unfiltered solution. The LS signal obtained for waxy maize starch solution filtered through a  $0.47 \mu\text{m}$  cellulose nitrate filter is very low due to the retention of high  $M_w$  fractions on the filter. However, the LS signal for corresponding waxy maize starch solutions filtered through  $8 \mu\text{m}$ ,  $5 \mu\text{m}$ ,  $3 \mu\text{m}$  and  $1 \mu\text{m}$  filters

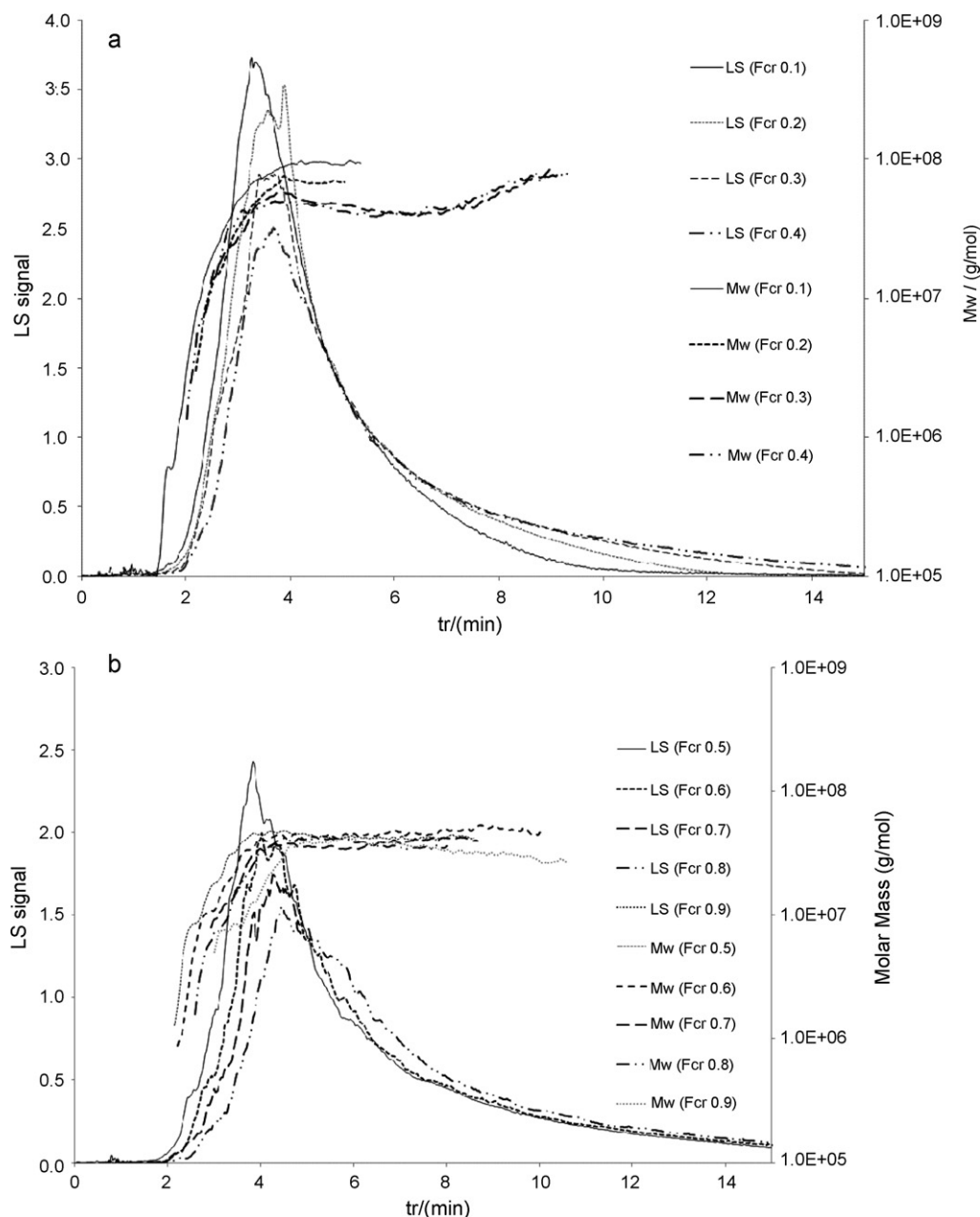


**Fig. 7.** (a)  $M_w$  as a function of  $t_r$  with LS peaks superimposed determined using the 2nd order Berry fit obtained for waxy maize starch at a fixed  $F_{ch}$  rate of 1.0 ml/min with  $F_{cr}$  rates ranging from 0.1 ml/min to 0.4 ml/min. (b)  $M_w$  as a function of  $t_r$  with LS peaks superimposed determined using the 2nd order Berry fit obtained for waxy maize starch at a fixed  $F_{ch}$  rate of 1.0 ml/min with  $F_{cr}$  rates ranging from 0.5 ml/min to 0.9 ml/min.

are unaffected. An 8  $\mu$ m cellulose nitrate filter was chosen to filter waxy maize starch solutions for AF4/MALS/RI analysis.

### 3.3. Analysis of light scattering data

The MALS data was evaluated using Eqs. (6) and (7) by plotting the excess Rayleigh scattering against  $\sin^2(\theta/2)$  at different angles ranging from 14° to 163°. Low angle detectors 14°, 26° and 35° were not included to process the results in some cases due to oversaturation. The Berry and Debye equations were found to provide the best fits to the light scattering data as shown in Fig. 3. The Berry method has been reported to be the most appropriate by others for starch (Bello-Perez, Roger, Baud, et al., 1998; Rolland-Sabate et al., 2007).

### 3.4. Effect of varying $F_{cr}$ rates upon LS and RI elution profiles

At a fixed  $F_{ch}$  of 1.0 ml/min,  $F_{cr}$  was varied from 0.1 to 1.0 ml/min in 0.1 ml/min increments. The retention time,  $t_r$ , was determined by subtracting the focusing time from the overall collection time. The LS and RI peaks as a function of retention time are shown in Figs. 4a, b and 5a, b, respectively. Both Figures show that the peaks become broader with increasing  $F_{cr}$  rates, due to the increase in retention time of the polymer molecules in the channel. The initial spike observed in the RI peak which appears from ~1 min to ~2 min (Fig. 5a and b) is due to the pressure drop in the transition from focusing to elution. Due to the low signal-to-noise ratio the pressure drop is more noticeable with RI peaks. The peak areas corresponding to the void peak and the RI spike were excluded for the determination of the molar mass and size measurements.

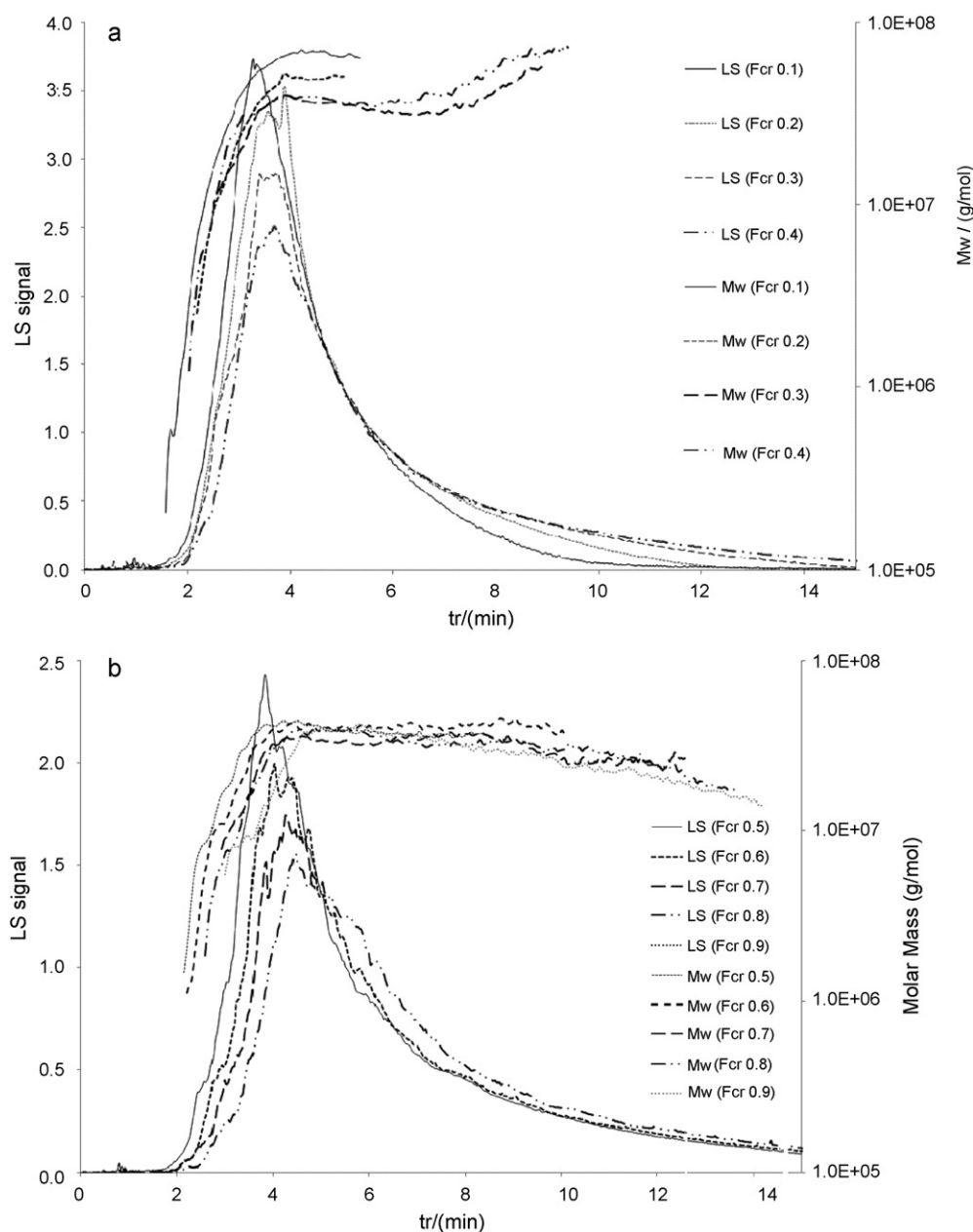


**Fig. 8.** (a)  $M_w$  as a function of  $t_r$  with LS peaks superimposed determined using the 3rd order Debye fit obtained for waxy maize starch at a fixed  $F_{ch}$  rate of 1.0 ml/min with  $F_{cr}$  rates ranging from 0.1 ml/min to 0.4 ml/min. (b)  $M_w$  as a function of  $t_r$  with LS peaks superimposed determined using the 3rd order Debye fit obtained for waxy maize starch at a fixed  $F_{ch}$  rate of 1.0 ml/min with  $F_{cr}$  rates ranging from 0.5 ml/min to 0.9 ml/min.

### 3.5. Average $M_w$ and $R_g$ values obtained with varying flow rates for waxy maize starch

The average  $M_w$  and  $R_g$  values of waxy maize starch obtained at a fixed  $F_{ch}$  rate of 1.0 ml/min with varying  $F_{cr}$  rates determined using Berry (1st and 2nd order) fits and 3rd order Debye fit are presented in Table 2. It should be noted that the errors generated by the ASTRA software quoted in Table 2, are not absolute and only represent the quality of the data collected. The LS data corresponding to low angles ( $14^\circ$  to  $48^\circ$ ) were excluded due to oversaturation (Table 2). The resultant  $M_w$  and  $R_g$  values are therefore prone to errors. The results show that  $M_w$  and  $R_g$  vary slightly with the LS fit model used. The values obtained are of the same order as reported by others using alternative dissolution procedures and measurement techniques which are summarized in Table 1.

The average  $M_w$  and  $R_g$  values of waxy maize starch determined with AF4/MALS/RI were found to be  $32 \times 10^6$  g/mol and 138 nm (1st order Berry fit) and  $37 \times 10^6$  g/mol and 164 nm (2nd order Berry fit), respectively. We obtained high mass recoveries ranging from 100% to 92% determined from the mass injected. A number of researchers have reported  $M_w$  values ranging from  $20 \times 10^6$  g/mol to over  $300 \times 10^6$  g/mol and  $R_g$  values ranging from 60 nm to over 300 nm as detailed in Table 1. The variation of the  $M_w$  and  $R_g$  values reported in the literature may arise from a number of factors including the source of waxy maize starch, the dissolution process, the analytical technique used and in the case of MALS the procedure used to process the light scattering data. Bowen et al. reported results using AF4/MALS/RI for waxy maize starch samples which were dispersed in water and treated in a pressure cell at  $140^\circ\text{C}$  for 10 min with an applied pressure of 4 bar in order to dissolve (2006). A  $M_w$  value of  $409 \times 10^6$  g/mol was determined which is considerably higher

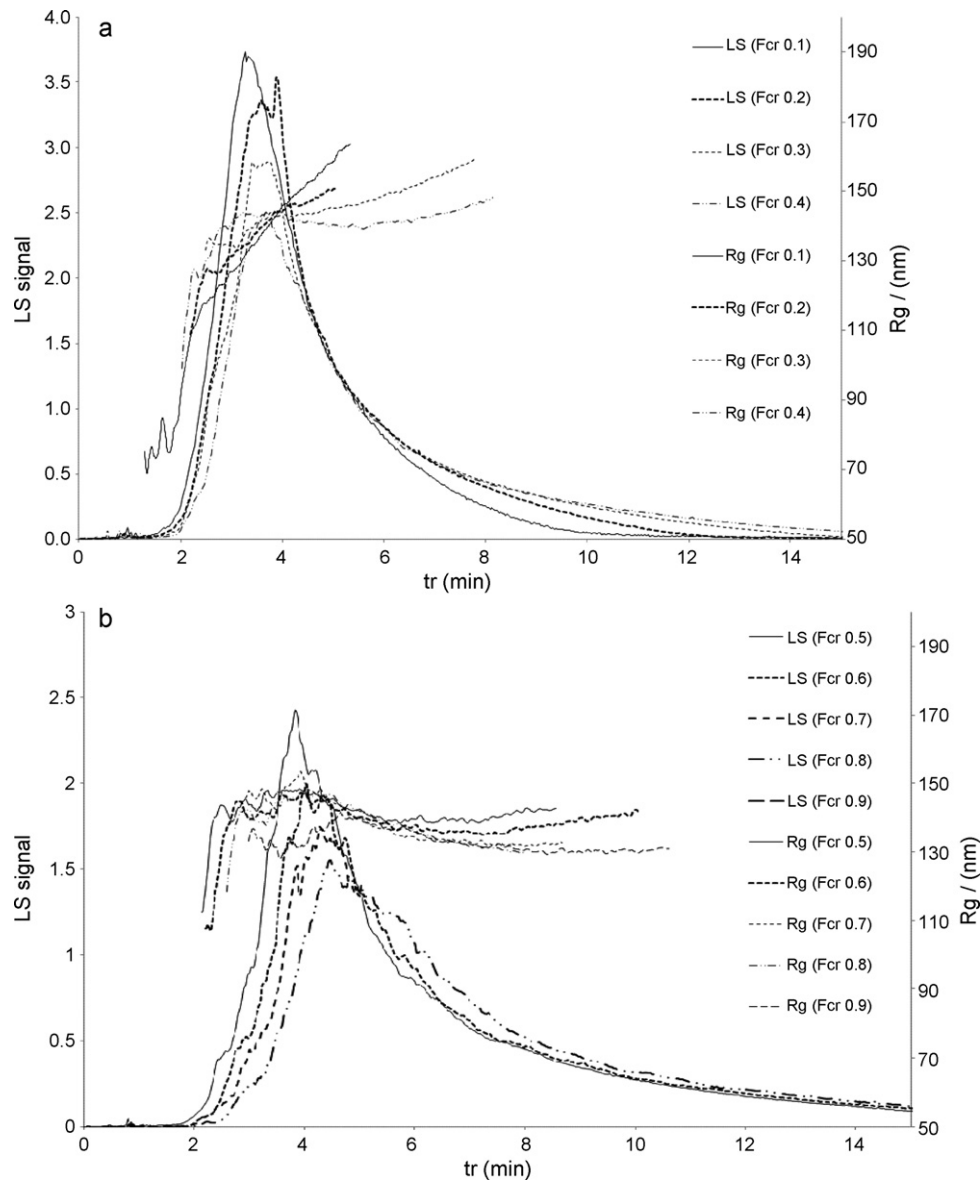


**Fig. 9.** (a)  $R_g$  as a function of  $t_r$  with LS peaks superimposed determined using the 1st order Berry fit obtained for waxy maize starch at a fixed  $F_{ch}$  rate of 1.0 ml/min with  $F_{cr}$  rates ranging from 0.1 ml/min to 0.4 ml/min. (b)  $R_g$  as a function of  $t_r$  with LS peaks superimposed determined using the 1st order Berry fit obtained for waxy maize starch at a fixed  $F_{ch}$  rate of 1.0 ml/min with  $F_{cr}$  rates ranging from 0.5 ml/min to 0.9 ml/min.

**Table 2**

Average  $M_w$  and  $R_g$  results for waxy maize starch obtained at fixed  $F_{ch}$  rate of 1.0 ml/min with varying  $F_{cr}$  rates determined using the 1st order Berry fit, the 2nd order Berry fit and the 3rd order Debye fit. The %error values generated by ASTRA software are given in brackets, which represents the quality of the data collected from LS detector and are not absolute errors.

$F_{cr}$ (ml/min)	LS detectors excluded	1st order Berry fit		2nd order Berry fit		3rd order Debye fit		% mass recovery
		$M_w$ (g/mol)	$R_g$ (nm)	$M_w$ (g/mol)	$R_g$ (nm)	$M_w$ (g/mol)	$R_g$ (nm)	
0.1	14°, 26°, 35° & 43°	$33 \times 10^6$ (3%)	141 (1%)	$41 \times 10^6$ (6%)	167 (3%)	$36 \times 10^6$ (3%)	119 (3%)	100
0.2	14°, 26°, 35° & 43°	$31 \times 10^6$ (4%)	140 (2%)	$41 \times 10^6$ (4%)	178 (2%)	$30 \times 10^6$ (3%)	121 (3%)	100
0.3	14°, 26°, 35° & 43°	$33 \times 10^6$ (4%)	146 (1%)	$42 \times 10^6$ (7%)	174 (3%)	$31 \times 10^6$ (2%)	120 (2%)	100
0.4	14° & 26°	$34 \times 10^6$ (4%)	142 (1%)	$39 \times 10^6$ (6%)	162 (3%)	$32 \times 10^6$ (3%)	120 (3%)	100
0.5	14° & 26°	$33 \times 10^6$ (3%)	144 (1%)	$38 \times 10^6$ (6%)	165 (3%)	$31 \times 10^6$ (2%)	120 (3%)	98
0.6	14° & 26°	$32 \times 10^6$ (4%)	141 (1%)	$37 \times 10^6$ (6%)	163 (3%)	$30 \times 10^6$ (3%)	120 (3%)	98
0.7	14° & 26°	$31 \times 10^6$ (4%)	140 (1%)	$35 \times 10^6$ (6%)	160 (3%)	$29 \times 10^6$ (3%)	118 (3%)	98
0.8	14° & 26°	$31 \times 10^6$ (4%)	138 (1%)	$34 \times 10^6$ (6%)	158 (3%)	$29 \times 10^6$ (3%)	117 (3%)	99
0.9	14° & 26°	$29 \times 10^6$ (5%)	134 (2%)	$34 \times 10^6$ (7%)	161 (3%)	$28 \times 10^6$ (3%)	118 (3%)	92
1.0	14°	$27 \times 10^6$ (4%)	135 (2%)	$28 \times 10^6$ (6%)	150 (3%)	$25 \times 10^6$ (3%)	115 (4%)	88



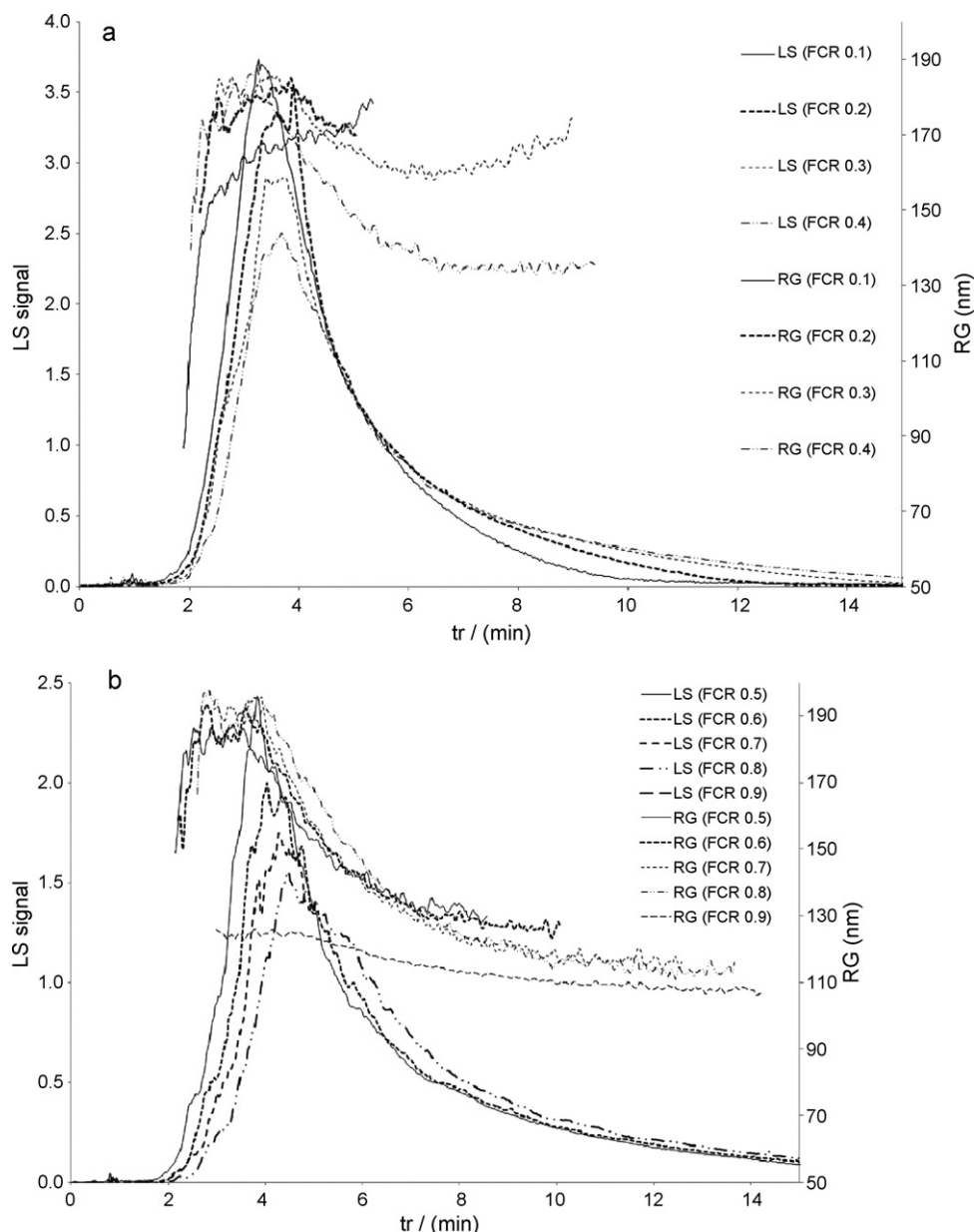


**Fig. 10.** (a)  $R_g$  as a function of  $t_r$  with LS peaks superimposed determined using the 2nd order Berry fit obtained for waxy maize starch at a fixed  $F_{ch}$  rate of 1.0 ml/min with  $F_{cr}$  rates ranging from 0.1 ml/min to 0.4 ml/min. (b)  $R_g$  as a function of  $t_r$  with LS peaks superimposed determined using the 2nd order Berry fit obtained for waxy maize starch at a fixed  $F_{ch}$  rate of 1.0 ml/min with  $F_{cr}$  rates ranging from 0.5 ml/min to 0.9 ml/min.

than values found in our work and by others. Rolland-Sabaté et al. also determined the  $M_w$  and  $R_g$  of waxy maize starch using a similar dissolution procedure to ours together with AF4/MALS/RI and reported values of  $318 \times 10^6 \text{ g mol}^{-1}$  and 228.9 nm, respectively (2007). van Bruijnsvoort et al. also determined the  $M_w$  distribution of waxy maize starch using aFFF coupled with MALS/RI detectors and also reported  $M_w$  values in excess of  $100 \times 10^6 \text{ g/mol}$  with  $R_g$  values over 300 nm (2001). Interestingly, they noted the presence of a steric/hyperlayer effect since they observed that  $R_g$  decreased rather than increased with elution time. In these studies the starch samples were simply prepared by heating in water and it is likely that they were not fully solubilised.

### 3.6. Effect of varying flow rates upon $M_w$ and $R_g$ distributions for waxy maize starch

The  $M_w$  distribution as a function of elution time for waxy maize starch obtained at a fixed  $F_{ch}$  rate of 1.0 ml/min and varying  $F_{cr}$

rates ranging from 0.1 ml/min to 0.9 ml/min, employing three different LS models: 1st order Berry (Fig. 6a and b), 2nd order Berry (Fig. 7a and b), and 3rd order Debye fit (Fig. 8a and b). Similar molar mass profiles for waxy corn starch were obtained with all three different LS fits. At a  $F_{cr}$  rate of 0.1 ml/min,  $M_w$  determined with the 1st order Berry fit increases sharply from  $\sim 1 \times 10^6 \text{ g/mol}$  to  $50 \times 10^6 \text{ g/mol}$  and then gradually increases to  $80 \times 10^6 \text{ g/mol}$ . Thereafter, it decreases to  $50 \times 10^6 \text{ g/mol}$ . Similar behaviour is seen with a  $F_{cr}$  rate of 0.2 ml/min. At high  $F_{cr}$  rates the  $M_w$  increases rapidly from  $\sim 5 \times 10^6 \text{ g/mol}$  to  $40 \times 10^6 \text{ g/mol}$  and then gradually increases to  $\sim 50 \times 10^6 \text{ g/mol}$ , after which it increases rapidly to  $\sim 70 \times 10^6 \text{ g/mol}$ . Similar  $M_w$  distributions were also obtained at a fixed  $F_{ch}$  rate of 0.5 ml/min with varying  $F_{cr}$  rates determined using the 1st order Berry fit, shown in Fig. 14. The separation of  $R_g$  as a function of  $t_r$  at a fixed  $F_{ch}$  rate of 1.0 ml/min with variable  $F_{cr}$  rates was determined with the 1st order Berry fit (Fig. 9a and b), the 2nd order Berry fit (Fig. 10a and b), and 3rd order Debye fit (Fig. 11a and b).

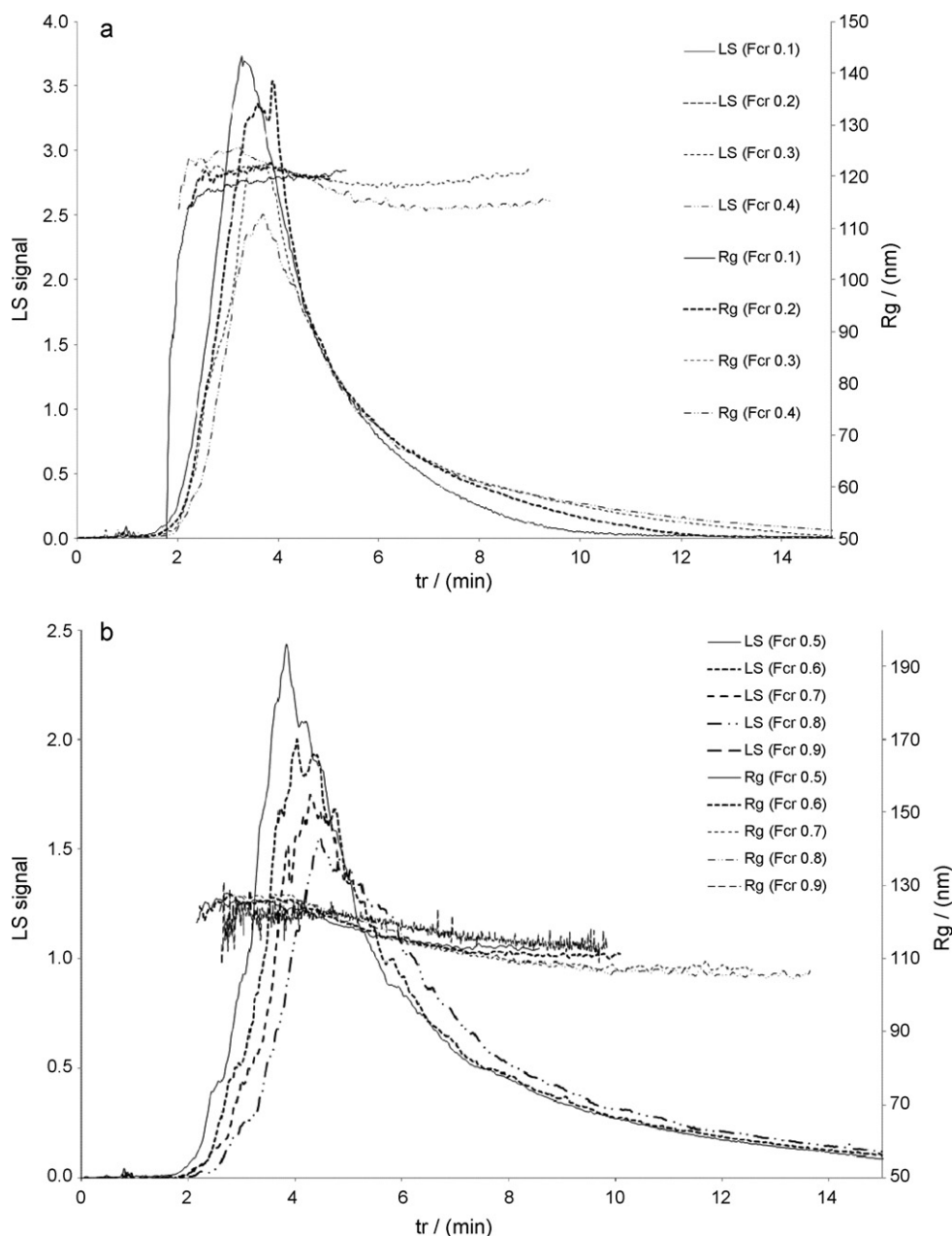


**Fig. 11.** (a)  $R_g$  as a function of  $t_r$  with LS peaks superimposed determined using the 3rd order Debye fit obtained for waxy maize starch at a fixed  $F_{ch}$  rate of 1.0 ml/min with  $F_{cr}$  rates ranging from 0.1 ml/min to 0.4 ml/min. (b)  $R_g$  as a function of  $t_r$  with LS peaks superimposed determined using the 3rd order Debye fit obtained for waxy maize starch at a fixed  $F_{ch}$  rate of 1.0 ml/min with  $F_{cr}$  rates ranging from 0.5 ml/min to 0.9 ml/min.

At a  $F_{cr}$  rate of 0.1 ml/min for waxy maize starch using the 1st order Berry fit,  $R_g$  was found to rise sharply from 70 nm to 120 nm and then gradually increases to 190 nm, as seen in Fig. 9a. At higher  $F_{cr}$  rates of 0.2–0.4 ml/min,  $R_g$  separation is hardly observed with  $R_g$  values ranging from 120 nm to 150 nm as shown in Fig. 9a.  $R_g$  separations obtained at lower  $F_{cr}$  rates determined with the 2nd order Berry fit (Fig. 10a) are similar to the ones obtained with 1st order Berry fit. At higher  $F_{cr}$  rates (0.5 ml/min to 0.9 ml/min) the  $R_g$  values initially do not change and slowly decrease afterwards. As with the 3rd order Debye fit no  $R_g$  separation is observed shown in Fig. 11a and b. Therefore, the 1st order Berry was found to be a suitable method for determining the  $M_w$  and  $R_g$  of waxy maize starch.

### 3.7. Effect of non-linear elution programmes upon the $M_w$ and $R_g$ distributions of waxy maize starch

Non-linear elution, such as gradient and exponential decay programmes in which the  $F_{ch}$  rate is constant and the  $F_{cr}$  rate lowers as a function of retention time, was used to analyse waxy maize starch.

At a fixed  $F_{ch}$  rate of 0.7 ml/min, the  $F_{cr}$  rate was decreased in a gradient fashion from 0.7 ml/min to 0.05 ml/min over 20 min. The LS and RI elution peaks with the  $M_w$  distribution and  $R_g$  superimposed, as shown in Figs. 12 and 13a and b, respectively. At a fixed  $F_{ch}$  rate of 0.7 ml/min, the  $F_{cr}$  rate was decreased exponentially from 0.7 ml/min to 0.05 ml/min over 20 min. The LS and RI

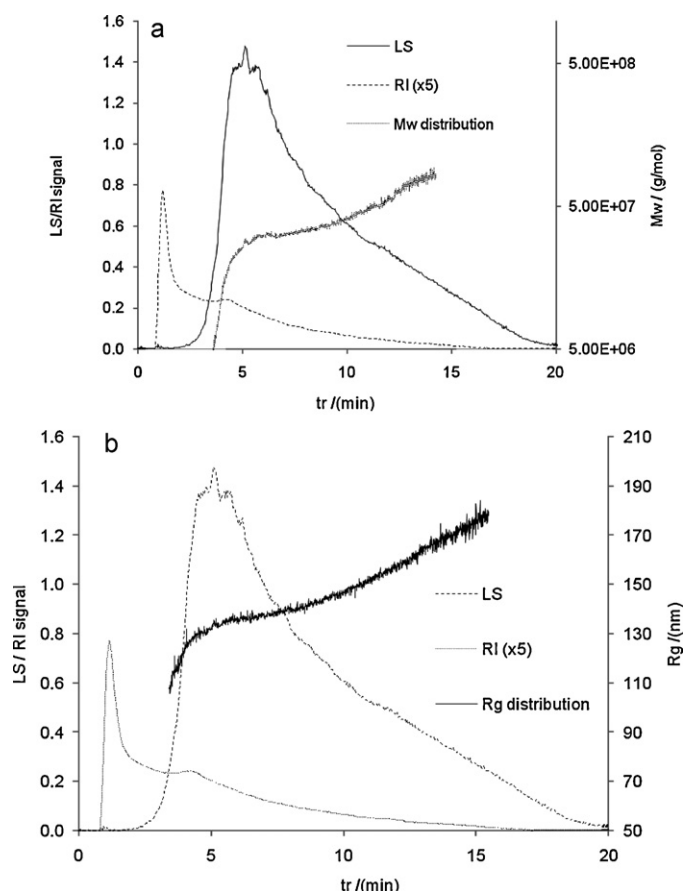


**Fig. 12.** (a) LS and RI peaks with the  $M_w$  distribution of waxy maize starch obtained at a fixed  $F_{ch}$  rate of 0.7 ml/min with  $F_{cr}$  rate varied from 0.7 ml/min to 0.05 ml/min in a gradient. (b) LS and RI peaks with the  $R_g$  distribution of waxy maize starch obtained at a fixed  $F_{ch}$  rate of 0.7 ml/min with  $F_{cr}$  rate varied from 0.7 ml/min to 0.05 ml/min in a gradient.

elution peaks with the  $M_w$  distribution superimposed is shown in Fig. 13a. The  $R_g$  distribution of waxy maize starch with LS and RI peaks superimposed is shown in Fig. 13b.

The majority of the sample eluted within 15 min with the gradient or exponential elution programme. The  $M_w$  rapidly increased from  $5 \times 10^6$  g/mol to  $45 \times 10^6$  g/mol, and then slowly increased to  $80 \times 10^6$  g/mol for both gradient and exponential decay programmes as seen in Figs. 12 and 13a, respectively.  $R_g$  of waxy maize starch increases gradually from  $\sim 100$  nm to 180 nm during gradient elution, as seen in Fig. 12b. Likewise, the  $R_g$  of waxy maize starch also increases gradually from  $\sim 110$  nm to 170 nm using an exponential decay elution programme as seen in Fig. 13b. The average molar mass and  $R_g$  values determined for waxy maize starch using the non-linear elution programmes are shown in Table 3. The average  $M_w$  and  $R_g$  values obtained with both gradient and exponential decay elution programmes are similar to the values obtained with linear elution programmes. Very high mass recover-

**Table 3**

Average molar mass and  $R_g$  values for waxy maize starch obtained with gradient and exponential decay programmes determined using the 1st order Berry fit. The % error values generated by ASTRA software is given in brackets and represent the quality of the LS detectors. LS data from low angles  $14^\circ$  and  $26^\circ$  were excluded from the determination of these results due to oversaturation.

Mode	$M_w$ (g/mol)	$R_g$ (nm)	% mass recovery
Gradient	$33 \times 10^6$ (5%)	149 (2%)	99
Exponential decay	$30 \times 10^6$ (5%)	146 (3%)	100

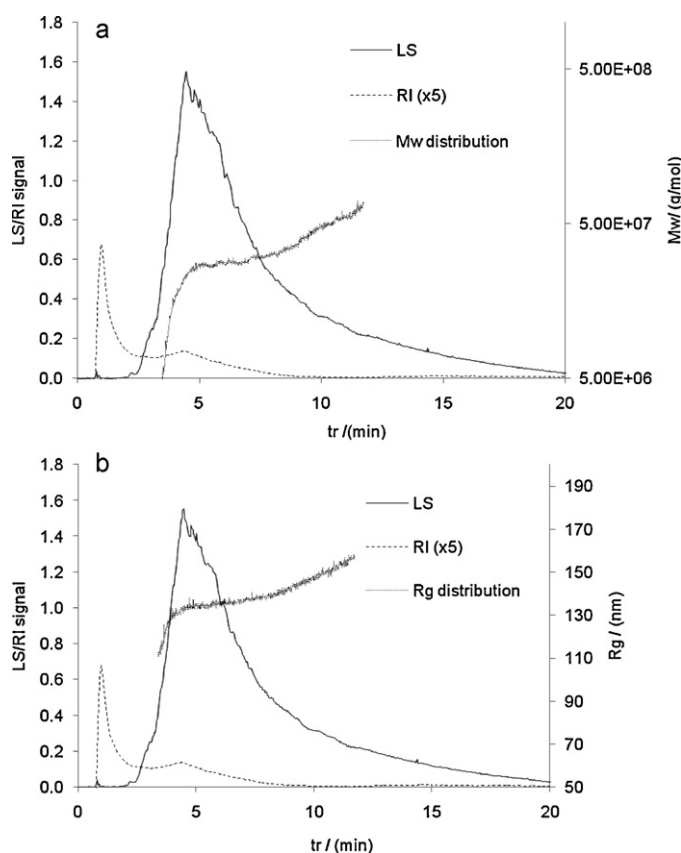


**Fig. 13.** (a) LS and RI peaks with the  $M_w$  distribution of waxy maize starch obtained at a fixed  $F_{ch}$  rate of 0.7 ml/min with  $F_{cr}$  rate decreased exponentially from 0.7 ml/min to 0.05 ml/min. (b) LS and RI peaks with the  $R_g$  distribution of waxy maize starch obtained at a fixed  $F_{ch}$  rate of 0.7 ml/min with the  $F_{cr}$  rate decreased exponentially from 0.7 ml/min to 0.05 ml/min.

ies were obtained with both gradient and exponential decay elution programmes.

### 3.8. Determination of $D$ and $R_h$ of waxy maize starch from aFFFF

The diffusion coefficient,  $D$  and the hydrodynamic radius,  $R_h$  of waxy maize starch were calculated from AF4 elution profiles obtained for waxy maize starch. The retention time  $t_r$  at the peak maxima of LS peaks for waxy maize starch was measured and the  $D$  and  $R_h$  was determined using the Stokes–Einstein relationship (Eqs. (1) and (4)). The  $D$  and  $R_h$  of waxy maize starch at fixed  $F_{ch}$  rates of 1.0 ml/min with varied  $F_{cr}$  rates are shown in Table 4.

The average  $D$  and  $R_h$  values range from  $1.4 \times 10^{-8}$  cm<sup>2</sup>/s to  $8.3 \times 10^{-8}$  cm<sup>2</sup>/s and 30 nm to 178 nm, respectively. Typically, at higher  $F_{cr}$  rates  $D$  increases and  $R_h$  decreases. The large molecules with low  $D$  are retained in the channel longer than the small molecules. At  $F_{cr}$  rates ranging from 0.2 ml/min to 0.4 ml/min the

**Table 4**

$D$  and  $R_h$  of waxy maize starch calculated from  $t_r$  at the peak maxima of LS peaks obtained at a fixed  $F_{ch}$  rate of 1.0 ml/min.

$F_{cr}$ (ml/min)	$t_r$ (min)	$D$ (cm <sup>2</sup> /s)	$R_h$ (nm)
0.1	3.2	$1.4 \times 10^{-8}$	178
0.2	3.4	$3.3 \times 10^{-8}$	76
0.3	3.5	$4.9 \times 10^{-8}$	52
0.4	3.6	$6.3 \times 10^{-8}$	40
0.5	3.8	$7.3 \times 10^{-8}$	35
0.6	4.0	$8.2 \times 10^{-8}$	31
0.7	4.2	$8.9 \times 10^{-8}$	28
0.8	4.4	$8.3 \times 10^{-8}$	30

**Table 5**

The conformation parameter ( $\alpha$ ,  $\beta$  and  $\gamma$ ) and linear regression  $R^2$  values obtained for waxy maize starch at a fixed  $F_{ch}$  rate of 0.5 ml/min and varied  $F_{cr}$  rates.

$F_{cr}$ (ml/min)	$\alpha$	$R^2$	$\beta$	$R^2$
0.1	0.23	0.992	0.29	0.992
0.2	0.26	0.989	0.33	0.997
0.3	0.26	0.996	0.30	0.988
0.4	0.21	0.997	0.32	0.975

average  $D$  values are in the region of  $\sim 5.0 \times 10^{-8}$  cm<sup>2</sup>/s and  $R_h$  values are  $\sim 60$  nm. These are similar to the  $D$  and  $R_h$  values determined with DLS of  $3.35 \times 10^{-8}$  cm<sup>2</sup>/s and 76 nm, respectively. Bello-Perez et al. (1996) reported a similar  $R_h$  value of 58 nm for waxy maize starch (Table 1).

### 3.9. Conformation of waxy maize starch

The conformation of the waxy maize starch molecules was determined using Eqs. (8) and (9).

$$D = C_1 M_w^{-\alpha} \quad (8)$$

$$R_g = C_2 M_w^{\beta} \quad (9)$$

$C_1$  and  $C_2$  are constants.  $\log D$  was plotted against the corresponding  $\log M_w$  values as shown in Fig. 14a. The values for the conformation parameter,  $\alpha$ , were determined from the slope as shown in Table 5. Similarly, the conformation parameter  $\beta$  was determined from the plot of  $\log R_g$  versus  $\log M_w$  as shown in Fig. 14b and Table 5. The values of the conformation parameters,  $\alpha$  and  $\beta$ , were found to be 0.2–0.33 indicative of a compact, spherical structure. Our findings are in agreement with the values reported by Fishman and Hoagland

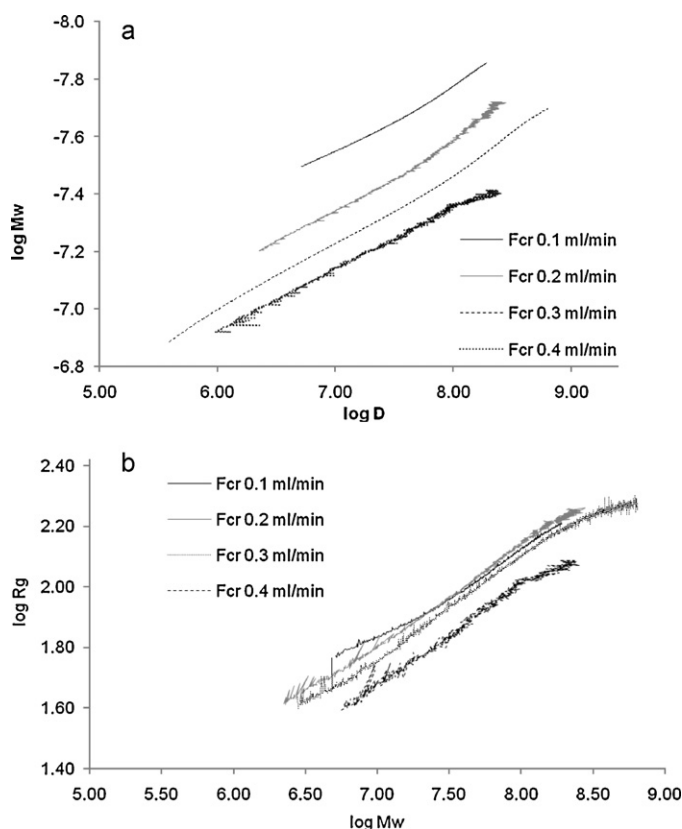


**Fig. 14.** (a)  $\log D$  plotted as a function of  $\log M_w$  for waxy maize starch at a fixed  $F_{ch}$  rate of 0.5 ml/min and varied  $F_{cr}$  rates. (b)  $\log R_g$  plotted as a function of  $\log M_w$  for waxy maize starch at a fixed  $F_{ch}$  rate of 0.5 ml/min and varied  $F_{cr}$  rates.

(1994), Bello-Perez et al. (1998a, 1998b) and Aberle et al. (1994).

### References

- Aberle, Th., Burchard, W., Vorwerg, W., & Radosta, S. (1994). Conformational contributions of amylose and amylopectin to the structural properties of starches from various sources. *Starch*, 46, 329–335.
- Andersson, M., Wittgren, B., & Wahlund, K.-G. (2001). Ultrahigh molar mass component detected in ethylhydroxyl cellulose by asymmetrical flow field-flow fractionation coupled to multi-angle light scattering. *Analytical Chemistry*, 73, 4852–4861.
- Andersson, M., Wittgren, B., & Wahlund, K.-G. (2003). Accuracy in multi-angle light scattering measurements for molar mass and radius estimations. Model calculations and experiments. *Analytical Chemistry*, 75, 4279–4291.
- Banks, W., & Greenwood, C. T. (1975). *Starch and its components*. Edinburgh (UK): Edinburgh University Press.
- Bello-Perez, L. A., Paredes-Lopez, O., Roger, P., & Colonna, P. (1996). Molecular characterization of some amylopectins. *Cereal Chemistry*, 73, 12–17.
- Bello-Perez, L. A., Roger, P., Baud, B., & Colonna, P. (1998). Macromolecular features of starches determined by aqueous high performance size exclusion chromatography. *Journal of Cereal Science*, 27, 267–268.
- Bello-Perez, L. A., Roger, P., Colonna, P., & Paredes-Lopez, O. (1998). Laser light scattering of high amylose and high amylopectin materials, stability in water after microwave dispersion. *Carbohydrate Polymers*, 37, 383–394.
- Bowen, S. E., Gray, D. A., Griaud, C., Majzoobi, M., Testa, C. E. M., Bello-Perez, L. A., et al. (2006). Lipid oxidation and amylopectin molecular weight changes occurring during storage of extruded starch samples. *Journal of Cereal Science*, 43, 275–283.
- Bultosa, G., Hamaker, B. R., & BeMiller, J. N. (2008). An SEC-MALLS study of molecular features of water-soluble amylopectin of Tef [Eragrostis tef (Zucc.) Trotter] starches. *Starch*, 60, 8–22.
- Cave, R. A., Seabrook, S. A., Gidley, M. J., & Gilbert, R. G. (2009). Characterization of starch by size exclusion chromatography: The limitations imposed by shear scission. *Biomacromolecules*, 10, 2245–2253.
- Elfstrand, L., Frigård, T., Roger, A., Eliasson, A.-C., Jönsson, M., Reslow, M., et al. (2004). Recrystallisation behaviour of native and processed waxy maize starch in relation to the molecular characteristics. *Carbohydrate Polymers*, 57, 389–400.
- Fishman, M. L., & Hoagland, P. D. (1994). Characterization of starches dissolved in water by microwave heating in a high pressure vessel. *Carbohydrate Polymers*, 23, 175–183.
- Fishman, M. L., Rodriguez, L., & Chau, H. K. (1996). Molar masses and sizes of starches by HPSEC-MALLS detection. *Journal of Agricultural Food Chemistry*, 44, 3182–3188.
- Gidley, M. J., Hanashiro, I., Hani, N. M., Hill, S. E., Huber, A., Jane, J.-L., et al. (2010). Reliable measurements of the size distributions of starch molecules in solution: Current dilemmas and recommendations. *Carbohydrate Polymers*, 79, 255–261.
- Han, J.-A., & Lim, S.-T. (2004a). Structural changes of corn starches by heating in DMSO measured by SEC-MALLS-RI system. *Carbohydrate Polymers*, 55, 265–272.
- Han, J.-A., & Lim, S.-T. (2004b). Structural changes in corn starches during alkaline dissolution by vortexing. *Carbohydrate Polymers*, 55, 193–199.
- Han, J.-A., Lim, H., & Lim, S.-T. (2005). Comparison between Size Exclusion Chromatography and Micro-Batch analyses of corn starches in DMSO using light scattering detector. *Starch*, 57, 262–267.
- Hanselmann, R., Burchard, W., Ehrat, M., & Widmer, H. M. (1996). Structural properties of fractionated starch polymers and their dependence of the dissolution process. *Macromolecules*, 29, 3277–3282.
- Jackson, D. S., Choto-Owen, C., Waniska, R. D., & Rooney, L. W. (1988). Characterisation of starch cooked in alkali by aqueous high performance size exclusion chromatography. *Cereal Chemistry*, 65, 493–496.
- Millard, M. M., Wolf, W. J., Dintzis, F. R., & Willet, J. L. (1999). The hydrodynamic characterisation of waxy maize amylopectin in 90% dimethyl sulfoxide–water by analytical centrifugation, dynamic and static light scattering. *Carbohydrate Polymers*, 39, 315–320.
- Modig, G., Nilsson, L., Bergensthal, B., & Wahlund, K.-G. (2006). Homogenization-induced degradation of hydrophobically modified starch determined by asymmetrical flow field-flow fractionation and multi-angle light scattering. *Food Hydrocolloids*, 20, 1087–1095.
- Murphy, P. (2000). In G. O. Phillips, & P. A. Williams (Eds.), *Handbook of hydrocolloids*. Cambridge (UK): Woodhead Publishers.
- Ratcliffe, I., Williams, P. A., Viebke, C., & Meadows, J. (2005). Physicochemical characterization of Konjac Glucomannan. *Biomacromolecules*, 6, 1977–1986.
- Roger, P., Baud, B., & Colonna, P. (2001). Characterisation of starch polysaccharides by flow field flow fractionation-multi-angle laser light scattering-differential refractometer index. *Journal of Chromatography A*, 917, 179–185.
- Roger, P., Bello-Perez, L. A., & Colonna, P. (1999). Contribution of amylose and amylopectin to the behaviour of starches in aqueous solution. *Polymer*, 40, 6897–6909.
- Rolland-Sabate, A., Colonna, P., Mendez-Montealvo, M. G., & Planhot, V. (2007). Branching features of amylopectins and glycogen determined by Asymmetrical Flow Field Flow Fractionation coupled with multiangle laser light scattering. *Biomacromolecules*, 8, 2520–2532.
- Stevenson, D. G., Biswas, A., Jane, Jay-Lin, & Inglett, G. E. (2007). Changes in Structure and properties of starch of four botanical sources dispersed in the ionic liquid 1-butyl-3-methylimidazolium chloride. *Carbohydrate Polymers*, 67, 21–31.

- Tetchi, F. A., Rolland-Sabate, A., Amani, G. N., & Colonna, P. (2007). Molecular and physicochemical characterisation of starches from Yam, Cassava, Sweet potato and ginger produced in the Ivory Coast. *Journal of the Science of Food and Agriculture*, 87, 1906–1916.
- van Bruijnsvoort, M., Wahlund, K.-G., Nilsson, G., & Kok, W. Th. (2001). Retention behaviour of amylopectins in Asymmetrical Flow Field-Flow Fractionation studied by multi-angle Light scattering detection. *Journal of Chromatography A*, 925, 171–182.
- Viebkke, C., & Williams, P. A. (2000). The influence of temperature on the characterisation of water-soluble polymers using asymmetrical flow field-flow fractionation, flow conditions of rapid elution. *Analytical Chemistry*, 72, 3896–3901.
- Vorwerg, W., & Radosta, S. (1995). Rheological investigation of starch polysaccharide. *Macromolecular Symposia*, 99, 71–82.
- Wahlund, K.-G. (2000). Asymmetrical Flow Field Flow Fractionation. In M. Schimpf, K. Caldwell, & J. C. Giddings (Eds.), *Field-Flow Fractionation handbook* (pp. 279–294). New York (USA): Wiley-Interscience.
- Wittgren, B., & Wahlund, K.-G. (1997). Fast molecular mass and size characterisation of polysaccharides using asymmetrical flow field-flow fractionation-multi-angle light scattering. *Journal of Chromatography A*, 760, 205–218.
- Yang, C., Meng, B., Chen, M., Liu, X., Hua, Y., & Ni, Z. (2006). Laser-light-scattering study of structure and dynamics of waxy corn amylopectin in dilute aqueous solution. *Carbohydrate Polymers*, 64, 190–196.
- Yoo, S.-H., & Jane, J.-L. (2002). Molecular weight and gyration radii of amylopectins determined by high-performance size-exclusion chromatography equipped with multi-angle laser-light scattering and refractive index detectors. *Carbohydrate Polymers*, 49, 307–314.